International Journal of Computational Engineering Science
Vol. 5, No. 4 (2004) 863–891

Imperial College Press
www.icpress.co.uk

# THE HYBRID BOUNDARY ELEMENT METHOD APPLIED TO PROBLEMS OF POTENTIAL THEORY IN NONHOMOGENEOUS MATERIALS

NEY A. DUMONT and RICARDO A. P. CHAVES

*Departamento de Engenharia Civil,*
*Pontifícia Universidade Católica do Rio de Janeiro,*
*Rua Marquês de São Vicente, 225, RJ 22453-900, Brazil*

GLAUCIO H. PAULINO

*Department of Civil and Environmental Engineering,*
*University of Illinois, Newmark Laboratory,*
*205 North Mathews Avenue Urbana, IL 61801-2352, USA*

Since the introduction of the hybrid boundary element method in 1987, it has been applied to various problems of elasticity and potential theory, including time-dependent problems. This paper focuses on establishing the conceptual framework for applying both the variational formulation and a simplified version of the hybrid boundary element method to nonhomogeneous materials. Several classes of fundamental solutions for problems of potential are derived. Thus, the boundary-only feature of the method is preserved even with a spatially varying material property. Several numerical examples are given in terms of an efficient patch test including irregularly bounded, unbounded, and multiply connected regions submitted to high gradients.

## 1. Introduction

The hybrid boundary element method, introduced in 1987 as a generalization of the concepts developed by Pian in the finite element method,[1–3] only requires evaluation of integrals along the boundary and uses fundamental solutions of the conventional boundary element method as domain interpolation functions. The method considers an arbitrarily shaped domain as a single finite macro-element with as many boundary degrees of freedom as desired. It also requires a flexibility matrix, for which evaluation of integrals along the entire boundary is required. The hybrid boundary element method has been applied to a wide variety of problems of potential and elasticity, including time-dependent problems and fracture mechanics.[4–7]

The present paper introduces a novel formulation – *the simplified hybrid boundary element method*[8–11] – which may be equally applied to nonhomogeneous media. In this simplified version, the time-consuming evaluation of the flexibility matrix $\mathbf{F}$ of the complete variational formulation is no longer required. However, as a price for the simplification, one gives up the complete variational consistency of the original method. As it shall be outlined, the equations of this method may be settled

on bases that are independent from all previously developed boundary element approaches.

A relevant area of application of this work consists of modeling functionally graded materials (FGMs) as nonhomogeneous materials. FGMs are special composites with a gradual transition in microstructure and composition, such as ceramic/ceramic (e.g. $MoSi_2/SiC$),[12] and metal/ceramic (e.g. Stainless steel/Zirconia) systems.[13] Such manufactured materials are suitable for a demanding array of new applications in severe loading environments – see, for example the book by Suresh and Mortensen [14], the book by Miyamoto et al. [15], and the review Chapter by Paulino et al. [16] Fundamental solutions play a paramount role in any boundary element formulation.[17] Deriving Green's functions for the elastic analysis of FGMs is hitherto an unbeaten challenge, except in some particular cases.[18,19] For problems of potential, on the other hand, solutions have been found for an exponentially varying physical parameter[20] and for more general variations, as previously done in the analysis of flow in nonhomogeneous medium. [21–24] A recent approach is the so called "simple BEM" by Sutradhar and Paulino [25], which has also been extended to transient problems. [26]

The remainder of this paper is organized as follows. For the sake of consistency with the present development, Sections 2-5 deal with the general outline of the hybrid boundary element method, as applied to problems of potential. Nevertheless, all theoretical considerations of this numerical method are equally valid, with some generalization and terminology adaptation, for elasticity problems.[2–6] By the way of terminology, it is worth remarking that some expressions, borrowed from the theory of elasticity, are used in the following Sections on problems of potential, as density energy, virtual work, stiffness matrix and flexibility matrix. This is done in an attempt to generalize concepts being used.

## 2. Basic Considerations on Fundamental Solutions

Consider the fundamental solution of a generic three-dimensional problem of potential, expressed in terms of the potential $u^*$ measured at a given point of a domain for some arbitrary, concentrated source $p^*_m$ (the subscript $m$ characterizes some location in the domain):

$$u^* = u^*_m p^*_m + u^c c \equiv (u^*_m + u^c C_m) p^*_m. \tag{1}$$

This fundamental solution, as characterized by the superscript "*", is usually given in the literature by the function $u^*_m$ alone, implicitly related to unitary sources $p^*_m$. The complete representation of Eq. (1) is adequate since it is stated for an arbitrary (not unitary) concentrated source $p^*_m$, and a term $u^c$ is added to take into account some arbitrary constant potential, as denoted by the superscript $c$. As indicated in the equation above, it may be convenient to correlate the arbitrary constant $c$ to concentrated sources $p^*_m$ by means of some arbitrary vector $C_m$ of constants.

In this paper, subscripts $m$ and $n$ refer to degrees of freedom of discretized quantities, and subscripts $i$ and $j$ refer to coordinate directions. A subscript after a comma denotes derivative with respect to the corresponding coordinate direction. Repeated indices indicate summation.

The fluxes at a given point of the domain are obtained from the potential as

$$q_i^* = -k_{ij} u^*{}_{,j}\,, \tag{2}$$

for some material physical parameters $k_{ij}$ that may vary spatially, as discussed in Section 7 for nonhomogeneous materials. One may formally write, in accordance with Eq. (1),

$$q_i^* = q_{im}^* p_m^* \text{ such that } q_i^*{}_{,i} = q_{im}^*{}_{,i}\, p_m^* = 0 \text{ in } \Omega, \tag{3}$$

as a property of a fundamental solution, for a domain $\Omega$ that does not include the points of application of $p_m^*$. If some domain $\Omega_0$ should comprise the point of application of a concentrated source $p_m^*$, then

$$\int_{\Omega_0} q_{im}^*{}_{,i}\, d\Omega = 1. \tag{4}$$

From the fluxes in Eq. (3) one obtains the normal fluxes along the boundary $\Gamma$ as

$$q_{im}^* \eta_i p_m^* = q_m^* p_m^*, \tag{5}$$

in which $\eta_j$ are the director cosines of the outward normal to the boundary.

The aim of the short outline above is to introduce some of the terminology needed in the remainder of the paper. As presented above, one is dealing with Green's functions, whose singularity is required to formulate an integral statement (as the Somigliana's identity in elasticity, basis of the conventional, collocation boundary element method). For the development of variational methods, on the other hand, a fundamental solution may be based on non-singular (polynomial) functions, as in Pian's[1] hybrid finite element method. However, the use of singular functions simplifies the whole formulation and ensures that the resultant matrix equations are well conditioned - although at the price of dealing with singular and improper integrals. The combination of singular, non-singular, and some special functions (as the Westergaard stress function in the fracture mechanics) may be of advantage when dealing with some particular stress gradients.[5]

## 3. Problem Formulation

Consider a body submitted to sources $b$ in the domain $\Omega$ and normal fluxes $\overline{q}$ on part $\Gamma_q$ of the boundary. The potential $\overline{u}$ is known on the complementary part $\Gamma_u$ of $\Gamma$. One is looking for an adequate approximation of the flux field that satisfies "equilibrium" both in the domain,

$$q_{i,i} = b \text{ in } \Omega, \tag{6}$$

and along part $\Gamma_q$ of the boundary,

$$q_i \eta_j = -\overline{q} \text{ along } \Gamma_q. \tag{7}$$

where $\eta_j$ denotes the j-th component of the normal vector. The corresponding potential must satisfy the boundary condition along $\Gamma_u$:

$$u = \overline{u} \text{ along } \Gamma_u. \tag{8}$$

A solution satisfying exactly all the three equations above is possible only in certain particular cases. In the present hybrid formulation, one assumes that a potential field

$$\widetilde{u} = u_m d_m \text{ such that } \widetilde{u} = \overline{u} \text{ along } \Gamma_u \tag{9}$$

is known along the boundary in terms of polynomial interpolation functions $u_m$ and some nodal potential parameters $d_m$, as usually done in other numerical methods. One also assumes a domain flux field $q_i^f$, with corresponding potential $u^f$,

$$\begin{aligned} q_i^f &= q_i^* + q_i^b \\ u^f &= u^* + u^b \end{aligned} \tag{10}$$

for the entire domain, in such a way that "equilibrium," Eq. (6), is identically satisfied. It means that one can define an arbitrary particular solution, $u^b$, such that the corresponding flux field $q_i^b$ satisfies the equation

$$q_i^b{}_{,i} = b \text{ in } \Omega \tag{11}$$

and, most important, it means that one can find a homogeneous solution $u^*$ with corresponding flux field $q_i^*$ that satisfies identically

$$q_i^*{}_{,i} = 0 \text{ in } \Omega. \tag{12}$$

This characterizes a fundamental solution, as introduced in Eq. (3), to be obtained in terms of some nodal source parameters, $p_m^*$, in which the subscript $m$ refers to each of the degrees of freedom of the discretized model.

## 4. Outline of the Hybrid Boundary Element Method

Given the considerations of Section 3, one shall look for a means of relating the fields $\widetilde{u}$, defined by Eq. (9) along $\Gamma$, and $u^f$, defined in $\Omega$ by Eqs. (10) - (12), in such a way that Eq. (7) is best satisfied. This may be achieved by means of a variational principle, as outlined in terms of the Hellinger-Reissner potential,

$$\begin{aligned} -\Pi_R(q_i^f, \widetilde{u}) = \int_\Omega \left[ U_0^C(q_i^f) - (q_i^f{}_{,i} - b)u \right] d\Omega + \\ \int_\Gamma q_i^f \eta_j \widetilde{u} d\Gamma + \int_{\Gamma_q} \widetilde{u} \overline{q}_i d\Gamma + \text{Const.}, \end{aligned} \tag{13}$$

as first applied by Pian to finite elements and here generalized for considering the flux field in the domain as a series of fundamental, singular solutions $q_i^f$, according to Eq. (10).[1-3]

The complementary density energy $U_0^C(q_i^f)$ of the equation above, as a function of the flux field, yields after integration by parts and application of Green's theorem the expression

$$\int_\Omega U_0^C(q_i^f)d\Omega = \mathbf{p}^{*\mathrm{T}}\left[\tfrac{1}{2}\mathbf{F}\mathbf{p}^* + \mathbf{b}^b\right] + \text{Const.}, \tag{14}$$

with the flexibility matrix $\mathbf{F}$ and the vector $\mathbf{b}^b$ of nodal potentials equivalent to the applied body sources,

$$\left[\mathbf{F} \;\; \mathbf{b}^b\right] = -\int_\Gamma q_{im}^* \eta_i \left\langle u_n^* \;\; u^b \right\rangle d\Gamma + \left\langle U_{mn}^* \;\; d_m^b \right\rangle, \tag{15}$$

expressed in a compact notation, in terms of only boundary integrals. In the equation above, $U_{mn}^*$ represents the potential evaluated at node $n$ for concentrated sources applied at node $m$. Similarly, $d_m^b$ is the body source potential evaluated at node $m$. Numerical implementation considerations of the matrix $\mathbf{F}$ shall be made opportunely. Observe that no constant potential appears in the expressions above, as a consequence of the fact that the flux of a fundamental solution is always in balance with the applied source:

$$\int_\Gamma q_{im}^* \eta_i d\Gamma + 1 \equiv 0. \tag{16}$$

Substituting in the Hellinger-Reissner potential of Eq. (13) the function $q_i^f$ for its expression according to Eqs. (10) and (5), the function $\widetilde{u}$ according to Eq. (9) and considering Eq. (14), one arrives at the matrix expression of the functional, already assumed as stationary,

$$-\delta\Pi_R = \delta\mathbf{p}^{*\mathrm{T}}\left[\mathbf{F}\mathbf{p}^* - \mathbf{H}\mathbf{d} + \mathbf{b}^b\right] + \delta\mathbf{d}^{\mathrm{T}}\left[\mathbf{p} - \mathbf{p}^b - \mathbf{H}^{\mathrm{T}}\mathbf{p}^*\right] = 0 \tag{17}$$

in which the two vectors of nodal fluxes $\mathbf{p}$ and $\mathbf{p}^b$, equivalent to applied normal fluxes $\overline{q}$ and body sources $q_i^b\eta_i$, respectively, are defined as

$$\left[\mathbf{p} \;\; \mathbf{p}^b\right] = \int_\Gamma u_m \left\langle \overline{q} \;\; -q_i^b\eta_i \right\rangle d\Gamma. \tag{18}$$

With respect to the term that takes into account the work of the external boundary fluxes $\overline{q}$ in the equation above, one considers that integration is carried out along $\Gamma$ instead of $\Gamma_q$ because, after variation, $\delta\widetilde{u} = 0$ along $\Gamma_u$, according to Eq. (9). In Eq. (17) one also defines the potential transformation matrix

$$\mathbf{H} \equiv H_{mn} = -\int_\Gamma q_{im}^* \eta_i u_n d\Gamma + \delta_{mn}. \tag{19}$$

This is the same double-layer potential matrix of the conventional, collocation boundary element method. Its evaluation according to the equation above, in spite of the singularity that arises when $m$ and $n$ refer to the same nodal point, is considered a standard procedure.

Noticing that the particular solution may be approximated on the boundary in terms of the assumed interpolation functions introduced in Eq. (9), for potential parameters $\mathbf{d}^b \equiv d_n^b$ given as potentials $u^b$ measured at nodal points $n$,

$$u^b \approx u_n d_n^b \text{ along } \Gamma, \tag{20}$$

one may express $\mathbf{b}^b$ of Eq. (15) as

$$\mathbf{b}^b = \mathbf{H}\mathbf{d}^b \tag{21}$$

and rewrite Eq. (17) in a way more convenient for the further developments:

$$-\delta\Pi_R = \delta\mathbf{p}^{*\mathrm{T}}\left[\mathbf{F}\mathbf{p}^* - \mathbf{H}(\mathbf{d} - \mathbf{d}^b)\right] + \delta\mathbf{d}^{\mathrm{T}}\left[\mathbf{p} - \mathbf{p}^b - \mathbf{H}^{\mathrm{T}}\mathbf{p}^*\right] = 0 \tag{22}$$

### 4.1. *Results for a simply connected domain – Matrix approach*

For the sake of better understanding the evaluation of the flexibility matrix $\mathbf{F}$, as defined in Eq. (15), it is convenient to express both matrices $\mathbf{F} \equiv F_{mn}$ and $\mathbf{H} \equiv H_{mn}$ in compact notation as

$$\left[\mathbf{F} \;\; \mathbf{H}\right] = -\int_\Gamma q_{im}^* \eta_i \left\langle u_n^* \;\; u_n \right\rangle d\Gamma + \left\langle U_{mn}^* \;\; \delta_{mn} \right\rangle. \tag{23}$$

Observe that the interpolation function $u_n$, introduced in Eq. (9), is by definition equal to unity when $m$ and $n$ refer to the same node, and equal to zero in the remaining nodal points.

Owing to the singularity of the fundamental solution, the boundary integrals represented by the equations above are singular and have to be split into Cauchy principal values and discontinuous terms. Elements about the main diagonal of the flexibility matrix $\mathbf{F}$, for $m$ and $n$ referring to the same node, cannot be evaluated by means of a standard integral, since singularities of the type $\ln(r)/r$, for two-dimensional problems, or $1/r^3$, for three-dimensional problems, arise as $r \to 0$. This mathematical feature is consistent with the assumption - common to all boundary element formulations - that the nodal point is situated outside the domain $\Omega$, although infinitely close to it, which means that the corresponding equivalent nodal potentials $F_{mn}$ are undetermined in terms of virtual work. The determination of these elements has to be carried out indirectly by investigating the physical meaning of the linear transformation carried out by $\mathbf{F}$ in the equations resulting from Eq. (22). In order to evaluate the off-diagonal terms of the flexibility matrix $\mathbf{F}$, Eq. (23) is split as follows

$$\begin{aligned}\left[\mathbf{F} \;\; \mathbf{H}\right] &\equiv \left[\mathbf{F}_{fp} \;\; \mathbf{H}_{fp}\right] + \left[\mathbf{F}_{disc} \;\; \mathbf{H}_{disc}\right] \\ &= -fp\int_\Gamma q_{im}^* \eta_i \left\langle u_n^* \;\; u_n \right\rangle d\Gamma + \\ &\quad \left(-\int_{\Gamma_0} q_{im}^* \eta_i \left\langle u_n^* \;\; u_n \right\rangle d\Gamma + \left\langle U_{mn}^* \;\; \delta_{mn} \right\rangle\right),\end{aligned} \tag{24}$$

in which *fp*, in general, denotes the finite part (a Cauchy principal value, in the case) and subscript *disc* refers to the discontinuous terms of the general, singular

integrals of Eq. (23). In this equation, $\Gamma_0$ is an arbitrarily small boundary that envelops the singularity point. For $m$ and $n$ referring to different nodal points, there are no singularities involved, which means that $\mathbf{H}_{disc}$ is a diagonal matrix for problems of potential (as well established in the literature). The main-diagonal elements of $\mathbf{H}$, corresponding to $\mathbf{H}_{disc}$ added to the main-diagonal elements of $\mathbf{H}_{fp}$, might be obtained indirectly by making use of the orthogonality criterion

$$\mathbf{HW} = \mathbf{0}, \tag{25}$$

in which $\mathbf{W}$ is, for convenience, a normalized basis of constant nodal potential, such that $\mathbf{WW}^{\mathrm{T}} = 1$, thus circumventing the explicit evaluation of $\mathbf{H}_{disc}$. However, for the complete evaluation of $\mathbf{F}$, one takes account of $\mathbf{H}_{disc}$, as defined in Eq. (24), and rewrites this equation as

$$\begin{aligned} \left[\mathbf{F} \;\; \mathbf{H}\right] &\equiv \left[\mathbf{F}_{fp} \;\; \mathbf{H}_{fp}\right] + \left[\mathbf{F}_{disc} \;\; \mathbf{H}_{disc}\right] \\ &= \left[\mathbf{F}_{fp} \;\; \mathbf{H}_{fp}\right] + \mathbf{H}_{disc}\left[\mathbf{U}^{*} \;\; \mathbf{I}\right], \end{aligned} \tag{26}$$

since, by construction,

$$-\int_{\Gamma_0} q^{*}_{im}\eta_i u^{*}_n d\Gamma + U^{*}_{mn} \equiv \mathbf{H}_{disc}\mathbf{U}^{*}. \tag{27}$$

The evaluation of the elements comprised by $\mathbf{F}_{fp}$ involves the same mathematical considerations as in the evaluation of $\mathbf{H}_{fp}$ in Eq. (24), added to improper-integral considerations related to $u^{*}_m$, as occurs in the evaluation of the single-layer potential matrix $\mathbf{G}$ of the conventional, collocation boundary element method. One sees, once more, in Eq. (26), that the main-diagonal elements of $\mathbf{F}$ cannot be evaluated in the frame of the integral equations of Eq. (23) – taken as unrelated matrices, both $\mathbf{F}_{fp}$ and $\mathbf{U} \equiv U^{*}_{mn}$ are undefined for $m$ and $n$ referring to the same nodal point.[27] This indeterminacy shall be adequately dealt with as follows.

Returning to the functional statement (22), one obtains for arbitrary variations, $\delta\mathbf{p}^{*}$ and $\delta\mathbf{d}$, two sets of equations:

$$\begin{aligned} \mathbf{Fp}^{*} &= \mathbf{H}(\mathbf{d} - \mathbf{d}^{b}) \\ \mathbf{H}^{\mathrm{T}}\mathbf{p}^{*} &= \mathbf{p} - \mathbf{p}^{b}. \end{aligned} \tag{28}$$

For a finite domain, the matrix $\mathbf{H}$ is singular by construction, as formalized in Eq. (25). As a consequence, there is a normal basis $\mathbf{V}$ (then, $\mathbf{VV}^{\mathrm{T}} = 1$) such that

$$\mathbf{H}^{\mathrm{T}}\mathbf{V} = \mathbf{0}. \tag{29}$$

Moreover, it may be verified that, by construction of Eqs. (18), in the second of Eqs. (28), one obtains

$$\mathbf{W}^{\mathrm{T}}\left(\mathbf{p} - \mathbf{p}^{b}\right) = \mathbf{0}. \tag{30}$$

As a consequence, one must have for physical consistency that also

$$\mathbf{V}^{\mathrm{T}}\mathbf{p}^{*} = \mathbf{0}, \tag{31}$$

from which follows, in the first of Eqs. (28), that, if $\mathbf{F}$ is singular, necessarily

$$\mathbf{FV} = \mathbf{0}. \tag{32}$$

This equation is the key for the evaluation of the main-diagonal elements of the matrix $\mathbf{F}$, which cannot be directly obtained by integration, as already discussed. One is tacitly assuming that, for a simply connected domain, $\mathbf{F}$ is singular. Mechanical considerations related to this assumption belong to the fundamentals of the hybrid boundary element method.

Considering the orthogonal properties given by Eqs. (31) and (32), one may solve the first of Eqs. (28) for $\mathbf{p}^*$, in terms of generalized inverses,[28] and introduce its expression into the second of Eqs. (28), thus arriving at the relation

$$\mathbf{H}^{\mathrm{T}} \left(\mathbf{F} + \mathbf{V}\mathbf{V}^{\mathrm{T}}\right)^{-1} \mathbf{H} \left(\mathbf{d} - \mathbf{d}^b\right) = \mathbf{p} - \mathbf{p}^b, \tag{33}$$

in which

$$\mathbf{K}_H \equiv \mathbf{H}^{\mathrm{T}} \left(\mathbf{F} + \mathbf{V}\mathbf{V}^{\mathrm{T}}\right)^{-1} \mathbf{H} \tag{34}$$

is a symmetric, positive semi-definite stiffness matrix. As a consequence of Eq. (25), this stiffness matrix is by construction orthogonal to constant nodal pontentials.

## 5. Outline of the Simplified Hybrid Boundary Element Method

In a simplified version, the time-consuming evaluation of the flexibility matrix $\mathbf{F}$ of last Section is no longer required. However, as a price for the simplification, one gives up the complete variational consistency of the original method. As it shall be outlined, the equations of this method may be settled on bases that are completely independent from all previously developed boundary element approaches,[8–11,27] although keeping conceptual affinity with the variational formulation just presented. In fact, as it will be outlined in Section 6, the extension of the (variational) hybrid boundary element method to unbounded regions and to multiply connected domains has become possible only after the full development of this simplified version.

### 5.1. *Nodal flux equilibrium in terms of virtual work*

A set of equations relating equivalent nodal fluxes acting on the boundary to the concentrated sources $\mathbf{p}^*$ was obtained as the second of Eqs. (28) in the frame of the hybrid boundary element method, based on the Hellinger-Reissner potential. However, a conceptually less involved approach suffices one's purpose in this Section to arrive at the same result. Given a virtual field of potential $\delta\widetilde{u}$, such that

$$\delta\widetilde{u} = 0 \text{ in } \Gamma_u, \tag{35}$$

Eqs. (6) and (7) are equivalent to the virtual work statement

$$\int_\Omega \left(q_i^* + q_i^b\right) \delta\widetilde{u}_{,i}\, d\Omega = -\int_\Omega b\delta\widetilde{u} d\Omega - \int_\Gamma \overline{q}\delta\widetilde{u} d\Gamma, \tag{36}$$

already assuming that the indicated boundary integration takes into account the work of the external boundary fluxes $\overline{q}$ carried out along $\Gamma$ instead of $\Gamma_q$, considering Eq. (35). Integration by parts of the term at the left-hand side of this equation and application of Green's theorem yield

$$\int_{\Gamma} q_i^* \eta_i \delta\widetilde{u} d\Gamma - \int_{\Omega} q_{i,i}^* \delta\widetilde{u} d\Omega = -\int_{\Gamma} \overline{q} \delta\widetilde{u} d\Gamma - \int_{\Gamma} q_i^b \eta_i \delta\widetilde{u} d\Gamma, \tag{37}$$

or, substituting for $\delta\widetilde{u}$ and $q_i^*$ according to Eqs. (9) and (3), respectively,

$$\delta d_n \left( \int_{\Gamma} q_{im}^* \eta_i u_n d\Gamma - \int_{\Omega} q_{im,i}^* u_n d\Omega \right) p_m^* = \delta d_n \left( -\int_{\Gamma} \overline{q} u_n d\Gamma - \int_{\Gamma} q_i^b \eta_i u_n d\Gamma \right). \tag{38}$$

Then, for arbitrary nodal potentials $\delta\mathbf{d} \equiv \delta d_n$ one obtains the matrix equilibrium equation of equivalent nodal fluxes

$$\mathbf{H}^{\mathrm{T}} \mathbf{p}^* = \mathbf{p} - \mathbf{p}^b, \tag{39}$$

exactly the second of Eqs. (28), in which the transpose of the potential transformation matrix $\mathbf{H}$ (defined in Eq. (19)) is an equilibrium matrix that transforms concentrated sources $\mathbf{p}^*$ into equivalent nodal fluxes $\mathbf{p} - \mathbf{p}^b$ (defined in Eqs. (18)). Observe that Eqs. (25) and (29)-(31) remain unchanged in the context of this Section.

### 5.2. *Nodal potential compatibility*

#### 5.2.1. *Evaluation of potential results in the domain*

In the hybrid boundary element method, the constant potential contribution has to be evaluated explicitly during post-analysis, as no reference has been made to the constants $C_m$ of Eq. (1). The consequences of the following developments are paramount for the extension of both versions of the hybrid boundary element methods to infinite domains. In a first step, one replaces $u^*$ in Eq. (10) with its expression in Eq. (1) and adds a constant potential $u^c c$, where $c$ is a potential parameter to be evaluated, thus resulting for the domain potential $u^f$:

$$u^f = u^* + u^b = (u_m^* + u^c C_m)\, p_m^* + u^b + u^c c. \tag{40}$$

The idea is to evaluate $C_m$, as carried out in Subsection 5.2.2, in such a way that $u_m^* + u^c C_m$ is orthogonal to constant potential and correlate $u^c c$ with the amount of constant potential given by the nodal values $\mathbf{d}$.[8,10,27] This way of expressing $u^f$ is consistent with the fact that, in the steady state case, the interaction between the primary unknowns of the problem - the concentrated nodal sources $\mathbf{p}^*$ and the nodal potentials $\mathbf{d}$ - does only occur in terms of balanced fluxes, as established by Eqs. (28). For the sake of simplicity, one expresses the constant potential $u^c$ in such a way that, when evaluated at the nodal points, it reproduces the normalized vector $\mathbf{W}$ of Eq. (25).[27]

Equation (40) is valid for the domain $\Omega$, as a consequence of the flux assumption therein, whereas Eq. (9) is assumed for the potential along the boundary $\Gamma$. However, one may enforce that both assumptions coincide at the nodal points,

$$\begin{aligned} \mathbf{d} &= (\mathbf{U}^* + \mathbf{WC})\,\mathbf{p}^* + \mathbf{d}^b + \mathbf{W}c \quad \text{or} \\ d_m &= (U^*_{mn} + W_m C_n)\,p^*_n + d^b_m + W_m c, \end{aligned} \tag{41}$$

in matrix and index notation, respectively. In this equation, $\mathbf{U}^*$ is a symmetric matrix obtained by expressing the fundamental solution $u^*_n$ at the nodal points, as already introduced in Eq. (24). When $m$ and $n$ refer to the same nodal point, the corresponding elements can be evaluated by means of a spectral property (to be explained opportunely). However, supposing that $\mathbf{U}^*$ is completely known, one obtains the constant potential parameter $c$ by pre-multiplying both sides of Eq. (41) by $\mathbf{W}^{\mathrm{T}}$ (recalling that $\mathbf{W}$ is normalized):

$$\begin{aligned} c &= \mathbf{W}^{\mathrm{T}}\left(\mathbf{d} - \mathbf{d}^b\right) - \left(\mathbf{W}^{\mathrm{T}}\mathbf{U}^* + \mathbf{C}\right)\mathbf{p}^* \quad \text{or} \\ c &= W_m\left(d_m - d^b_m\right) - \left(W_m U^*_{mn} + C_n\right)p^*_n. \end{aligned} \tag{42}$$

Now, substituting this expression into Eq. (40), one obtains the final expression of displacements at an interior point:

$$u^f = \left(u^*_m - u^c W_n U^*_{nm}\right)p^*_m + u^b + u^c W_m\left(d_m - d^b_m\right). \tag{43}$$

Observe that the vector $C_n$ of constants cancels out in this equation, which is a substitute for Eq. (40). However, Eq. (43) is still incomplete, as the elements of the matrix $\mathbf{U}^* \equiv U^*_{nm}$ cannot be directly obtained for $m$ and $n$ referring to the same node. Nonetheless, one applies Eq. (43) to the nodal points, again, to obtain

$$(\mathbf{I} - \mathbf{WW}^{\mathrm{T}})(\mathbf{d} - \mathbf{d}^b) = (\mathbf{I} - \mathbf{WW}^{\mathrm{T}})\mathbf{U}^*\mathbf{p}^*, \tag{44}$$

which is equivalent to Eq. (41). However, the latter equation is conceptually superior to the former one, as it is explicitly stated that, because of the orthogonal projector $(\mathbf{I} - \mathbf{WW}^{\mathrm{T}})$, only a potential field orthogonal to constant potential is transformed, in accordance with Eq. (39), which only transforms balanced fluxes.

### 5.2.2. *Main-diagonal elements of the matrix of potentials* $\mathbf{U}^*$

Although the vector $\mathbf{C}$ does not take part in the final expression of $u^f$ in Eq. (43), it can be evaluated, as a means of indirectly obtaining the unknown terms about the main diagonal of $U^*_{nm}$. Because $\mathbf{p}^*$ in Eqs. (28) stands for balanced fluxes (according to Eq. (31)), the term in brackets in Eq. (40) may be enforced to be orthogonal to a constant field. A reasonable orthogonality criterion is

$$\int_\Gamma u^c\left(u^*_m + u^c C_m\right)d\Gamma p^*_m = 0, \tag{45}$$

for any $p^*_m$, which leads to, in matrix notation,

$$\mathbf{C}^* + \mathbf{C}^c\mathbf{C} = 0 \implies \mathbf{C} = -(\mathbf{C}^c)^{-1}\mathbf{C}^*, \tag{46}$$

in which

$$\mathbf{C}^c = \int_\Gamma u^c u^c d\Gamma \quad \text{and} \quad \mathbf{C}^* \equiv C_m^* = \int_\Gamma u^c u_m^* d\Gamma. \tag{47}$$

Now, if the term in brackets in Eq. (41) is orthogonal to constant potentials, the orthogonality criterion (to unbalanced fluxes)

$$(\mathbf{U}^* + \mathbf{WC})\,\mathbf{V} = \mathbf{0} \tag{48}$$

must hold, according to Eq. (31). Moreover, Eq. (48) is the criterion needed for evaluating the elements of $\mathbf{U}^*$, when $m$ and $n$ refer to the same node.[8,27] For problems of potential, this equation results in a set of uncoupled equations for each diagonal element of $\mathbf{U}^*$. Consequently, absolute potential results at internal points can be evaluated according to Eq. (43), which is equivalent to Eq. (40) for $\mathbf{C} \equiv C_m$ given by Eq. (46).

### 5.3. *A stiffness-type matrix*

Equations (44) and (39), here gathered as a governing set of equations,

$$\begin{aligned} &(\mathbf{I} - \mathbf{WW}^{\mathrm{T}})\mathbf{U}^*\mathbf{p}^* = (\mathbf{I} - \mathbf{WW}^{\mathrm{T}})(\mathbf{d} - \mathbf{d}^b) \\ &\mathbf{H}^{\mathrm{T}}\mathbf{p}^* = \mathbf{p} - \mathbf{p}^b, \end{aligned} \tag{49}$$

are the required relations between nodal fluxes and potentials for the formulation of a general problem of potential. Observe that only potentials orthogonal to a constant field and balanced fluxes, according to Eqs. (30) and (31), are transformed. Moreover, it is straightforward to obtain from Eq. (48) that, consistently with Eq. (29),

$$(\mathbf{I} - \mathbf{WW}^{\mathrm{T}})\mathbf{U}^*\mathbf{V} = \mathbf{0}. \tag{50}$$

Solving for $\mathbf{p}^*$ in the first of Eqs. (49), one obtains, in terms of a Bott-Duffin inverse,[28]

$$\mathbf{p}^* = (\mathbf{I} - \mathbf{VV}^{\mathrm{T}})\left[(\mathbf{I} - \mathbf{WW}^{\mathrm{T}})\mathbf{U}^* + \mathbf{VV}^{\mathrm{T}}\right]^{-1}(\mathbf{I} - \mathbf{WW}^{\mathrm{T}})(\mathbf{d} - \mathbf{d}^b), \tag{51}$$

which, when substituted into the second of Eqs. (49), leads to the flux-potential relation

$$\mathbf{H}^{\mathrm{T}}\left[(\mathbf{I} - \mathbf{WW}^{\mathrm{T}})\mathbf{U}^* + \mathbf{VV}^{\mathrm{T}}\right]^{-1}(\mathbf{I} - \mathbf{WW}^{\mathrm{T}})(\mathbf{d} - \mathbf{d}^b) = \mathbf{p} - \mathbf{p}^b, \tag{52}$$

with the stiffness-type matrix

$$\mathbf{K}_{SH} = \mathbf{H}^{\mathrm{T}}\left[(\mathbf{I} - \mathbf{WW}^{\mathrm{T}})\mathbf{U}^* + \mathbf{VV}^{\mathrm{T}}\right]^{-1}(\mathbf{I} - \mathbf{WW}^{\mathrm{T}}). \tag{53}$$

Since the first of Eqs. (49) is formulated on the basis of a non-variational approach, $\mathbf{K}_{SH}$ is not necessarily symmetric. However, $\mathbf{K}_{SH}$ tends to become symmetric with increasing mesh refinement.[27] With slight modifications, the formulation of this paper is also valid for infinite domains (see next Section).

## 6. Unbounded Regions

The feasibility of both variational (Section 4) and simplified (Section 5) hybrid boundary element methods relies on the possibility of evaluating the main-diagonal elements of matrices $\mathbf{F}$ and $\mathbf{U}^*$, according to the orthogonality Eqs. (32) and (48), respectively. However, this is only possible if all elements of $\mathbf{V}$ are different from zero. It may be demonstrated that this is always the case for a simply connected, finite domain.[27] For the consideration of infinite domains, on the other hand, the orthogonality equations are not directly applicable because one can exclude neither a constant potential nor unbalanced fluxes from the energy considerations when dealing with this topologically different problem.

Fortunately, there are some simple relations between the matrices obtained for a cavity in an infinite domain and the corresponding matrices for the complementary bounded domain. First of all, observe that, in case of an unbounded domain, one simply writes for the potential

$$u^f = u^* + u^b = u^*_m p^*_m + u^b, \tag{54}$$

with some amount of constant potential that is implicit in the formulation and cannot be evaluated. Then, characterizing the matrices for an infinite domain with an upper bar ($^-$), it is possible to demonstrate following relations, given that one simply reverses the sense of integration in Eqs. (23), as well known in the literature on boundary element methods:[8]

$$\overline{\mathbf{H}} = \mathbf{I} - \mathbf{H}, \quad \overline{\mathbf{F}} = \mathbf{U}^* - \mathbf{F}, \tag{55}$$

in which $\mathbf{I}$ is the identity matrix. From the first of the equations above, together with Eq. (25), one readily obtains

$$\overline{\mathbf{H}}\mathbf{W} = \mathbf{W}, \tag{56}$$

which is a well known result in the boundary element literature. It is the counterpart of Eq. (25) for unbounded regions. For the flexibility matrix, on the other hand, one first adds the product $\mathbf{WC}$, for $\mathbf{C}$ given according to Eqs. (45) - (47), to both sides of the second of Eqs. (55):

$$(\overline{\mathbf{F}} + \mathbf{WC}) = (\mathbf{U}^* + \mathbf{WC}) - \mathbf{F}. \tag{57}$$

Then, multiplying all terms of this equation by $\mathbf{V}$, it follows from Eqs. (32) and (48) that

$$(\overline{\mathbf{F}} + \mathbf{WC})\mathbf{V} = \mathbf{0}, \tag{58}$$

which is the orthogonality condition required to evaluate the main-diagonal elements of the non-singular matrix $\overline{\mathbf{F}}$.

As a consequence, one obtains the sets of equations for unbounded domains, in both variational and simplified versions of the hybrid boundary element method:

$$\begin{aligned} \overline{\mathbf{F}}\mathbf{p}^* &= \overline{\mathbf{H}}(\mathbf{d} - \mathbf{d}^b) \\ \overline{\mathbf{H}}^{\mathrm{T}}\mathbf{p}^* &= \overline{\mathbf{p}} - \overline{\mathbf{p}}^b, \end{aligned} \tag{59}$$

and

$$\begin{aligned} (\mathbf{I} - \mathbf{W}\mathbf{W}^{\mathrm{T}})\mathbf{U}^*\mathbf{p}^* &= (\mathbf{I} - \mathbf{W}\mathbf{W}^{\mathrm{T}})(\mathbf{d} - \mathbf{d}^b) \\ \overline{\mathbf{H}}^{\mathrm{T}}\mathbf{p}^* &= \overline{\mathbf{p}} - \overline{\mathbf{p}}^b. \end{aligned} \tag{60}$$

Equation (58) shows that the variational and the simplified versions of the hybrid boundary element method, as presented in this paper, are interrelated. Some more conceptual considerations on these methods and other boundary element methods are reviewed in Dumont.[29]

In the case of a multiply connected domain, Eqs. (32) and (48) are no longer applicable, as it may be demonstrated that singularities or strong ill conditioning related to $\mathbf{V}$ unavoidably occur, for nodal points along interior subboundaries, physically explainable as a topological lack of correspondence between the bases $\mathbf{W}$ and $\mathbf{V}$. The theoretical discussion of this subject belongs to the fundamentals of the hybrid boundary element method. Nevertheless, the present method can be applied to a multiply connected domain, if one deals with the problem by superposing solutions for finite and infinite domains. Two numerical examples in Section 8 illustrate this possibility.

## 7. Fundamental Solutions for Nonhomogeneous Materials: Problems of Potential

In the following brief outline, one shall derive fundamental solutions for problems of potential that enable considering material properties varying according to three different patterns. A seemingly exhaustive development with the same goal, as applied to heterogeneous flows, has already been done by Cheng,[23,24] on the basis of previous theoretical achievements by Georghitza.[21,22] However, the developments of this Section have been carried out independently and according to an approach that enables a better understanding of material grading possibilities.[30,31] The next step should be the identification of problems and FGMs that could be dealt with on the basis of these fundamental solutions.

### 7.1. *Governing equations*

The present development, as applicable in the frame of the hybrid boundary element method, relies exclusively on real-variable functions. Time-independent problems are considered, with material properties varying in the direction $z$. This is illustrated in Fig. 1, for the case of two-dimensional problems. As given in the figure, the problem is described in terms of global coordinates $(X, Y, Z)$ and one is looking for

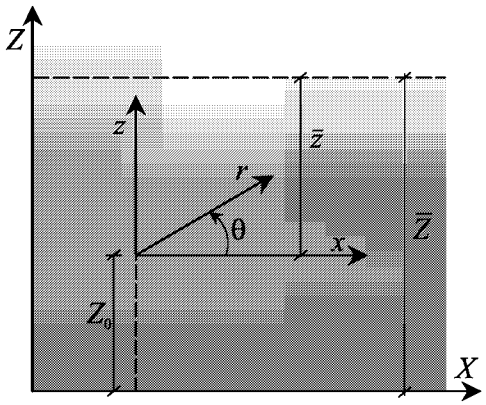


Fig. 1. Coordinate systems for the description of an FGM with material property $\overline{k}$ defined at $Z = \overline{Z}$ (global reference), which is equivalent to $z = \overline{z}$ (local reference).

a fundamental solution referred to local coordinates $(x, y, z)$, which shall eventually be changed to either cylindrical or polar coordinates, for the sake of solving the resulting governing differential equations.

For a steady state isotropic problem, the flux equation, for potential $u^* \equiv u^*(x, y, z)$, is

$$q_i = -k(z)u^*{}_{,i}\,, \tag{61}$$

in which $k(z)$ is the material physical parameter (thermal conductivity, for example). As illustrated in Fig. 1, $\overline{Z}$ is the global coordinate $Z$ of some reference value $\overline{k}$ for $k(z)$ corresponding to $\overline{z}$ in local coordinates $(x, y, z)$.

The flux balance equation of the problem, in absence of body sources, reads

$$q_{i,i} = 0. \tag{62}$$

Then, it follows from Eq. (61)

$$ku^*{}_{,ii} + k_{,z}\,u^*{}_{,z} = 0, \tag{63}$$

or

$$u^*{}_{,ii} + \frac{k_{,z}}{k}u^*{}_{,z} = 0. \tag{64}$$

7.1.1. *Governing equation for 3D problems*

Let's consider a solution $u^* \equiv u^*(x, y, z)$ of Eq. (64) in cylindrical coordinates $(\rho, \theta, z)$ that is independent from the angular coordinate $\theta$, thus satisfying

$$u^*{}_{,\rho\rho} + \frac{1}{\rho}u^*{}_{,\rho} + u^*{}_{,zz} + \frac{k_{,z}}{k}u^*{}_{,z} = 0. \tag{65}$$

Expressing the potential $u^*$ as the product

$$u^* = h(r)p(z) \tag{66}$$

and writing $r = \sqrt{\rho^2 + z^2}$ for the radius, one obtains for Eq. (64), after some manipulation,

$$h_{,rr} + \frac{2}{r} h_{,r} + h_{,r} \left( \frac{k_{,z}}{k} + 2\frac{p_{,z}}{p} \right) \frac{z}{r} + h \left( \frac{p_{,zz}}{p} + \frac{k_{,z}}{k} \frac{p_{,z}}{p} \right) = 0. \tag{67}$$

7.1.2. *Governing equation for 2D problems*

Let's consider a solution $u^* \equiv u^*(x, z)$ of Eq. (64) in polar coordinates $(r, \theta)$

$$u^*{}_{,rr} + \frac{1}{r} u^*{}_{,r} + \frac{1}{r^2} u^*{}_{,\theta\theta} + \frac{k_{,z}}{k} \left( u^*{}_{,r} \sin\theta + u^*{}_{,\theta} \frac{\cos\theta}{r} \right) = 0, \tag{68}$$

as

$$u^*{}_{,z} = u^*{}_{,r} \sin\theta + u^*{}_{,\theta} \frac{\cos\theta}{r}. \tag{69}$$

Expressing the potential $\theta$ as the product

$$u^* = h(r) p(r \sin\theta), \tag{70}$$

one obtains for Eq. (68), after some manipulation,

$$h_{,rr} + \frac{1}{r} h_{,r} + h_{,r} \left( \frac{k_{,z}}{k} + 2\frac{p_{,z}}{p} \right) \frac{z}{r} + h \left( \frac{p_{,zz}}{p} + \frac{k_{,z}}{k} \frac{p_{,z}}{p} \right) = 0. \tag{71}$$

## 7.2. *Solution of the governing equations* (67) *and* (71)

For consistency of both Eqs. (67) and (71), the following terms, expressed as functions of $z$, must be constant:

$$\left( \frac{p_{,zz}}{p} + \frac{k_{,z}}{k} \frac{p_{,z}}{p} \right) = A = \text{Const. and } \left( \frac{k_{,z}}{k} + 2\frac{p_{,z}}{p} \right) z = B = \text{Const.} \tag{72}$$

Then, six particular cases may be envisaged, in principle, for the sake of arriving at feasible variation patterns for the material property $k(z)$, as the constant $A$ may be negative, positive or equal to zero and the constant $B$ may be equal to or different from zero, as outlined in the two first columns of Table 1.

7.2.1. *First case: solution of the governing equations for* $A = -\beta^2 < 0, B = 0$

This assumption leads to the most frequently grading pattern suggested in the literature on FGMs[16]:

$$\begin{aligned} &\frac{p_{,zz}}{p} + \frac{k_{,z}}{k} \frac{p_{,z}}{p} = -\beta^2 \\ &\frac{k_{,z}}{k} + 2\frac{p_{,z}}{p} = 0. \end{aligned} \tag{73}$$

The general solution of these equations is

$$k = k_0 e^{-2\beta Z}\left(\alpha e^{2\beta Z}+1\right)^2 \text{ with } k_0 = \overline{k} e^{2\beta \overline{Z}}\left(\alpha e^{2\beta \overline{Z}}+1\right)^{-2}$$
$$p = p_0 e^{\beta Z}\left(\alpha e^{2\beta Z}+1\right)^{-1} \text{ with } p_0 = k_0^{-1} e^{\beta Z_0}\left(\alpha e^{2\beta Z_0}+1\right)^{-1}, \tag{74}$$

in terms of material constants $\alpha$, $\beta$ and $\overline{k}$. The constant $k_0$ is expressed in such a way that $k(\overline{z}) = \overline{k}$, the physical parameter of the reference layer. Moreover, $k(z)$ is intentionally expressed as a function of $Z \equiv z + Z_0$, in order to always represent the same material description regardless of local coordinate reference, according to Fig. 1. The parameter $p_0$ is best assessed after the considerations concerning $h(r)$.

According to the assumptions made in Eq. (73) for the terms in brackets in Eqs. (67) and (71), the function $h(r)$ is solved as

$$h_{,rr} + \frac{2}{r} h_{,r} - \beta^2 h = 0 \Longrightarrow h = \frac{C_1 \cosh(\beta r) + C_2 \sinh(\beta r)}{r} \text{ for 3D problems,} \tag{75}$$

$$h_{,rr} + \frac{1}{r} h_{,r} - \beta^2 h = 0 \Longrightarrow h = C_1 \mathrm{K}_0(\beta r) + C_2 \mathrm{I}_0(\beta r) \text{ for 2D problems,} \tag{76}$$

where $\mathrm{I}_0$ and $\mathrm{K}_0$ are modified Bessel functions of order zero. The, in principle, arbitrary integration constants in the solution of either function $h(r)$ are evaluated in such a way that

$$h = \frac{-\cosh(\beta r)}{4\pi r} \text{ for 3D problems,} \tag{77}$$

$$h = \frac{1}{2\pi}\left\{\mathrm{K}_0(\beta r) + \left[\ln(\frac{\beta}{2}) + \gamma\right]\mathrm{I}_0(\beta r)\right\} \text{ for 2D problems,} \tag{78}$$

in order to correspond to a unitary concentrated source applied at $r = 0$, regardless of the value of $\beta$, and to arrive at the homogeneous solution as $\beta \to 0$.

The potential function $u^* = h(r)p(z)$, as given by Eqs. (66) or (70), for 3D or 2D problems, respectively, also must correspond to a unitary singular source at $r = 0$, regardless of the fact that one is dealing with a non-homogeneous material. This is the way to evaluate $p_0$, as given in the second row of Eqs. (74), for both 3D and 2D cases.

Instead of Eqs. (74), one may write the more restrictive solution of Eqs. (73), corresponding to $\alpha = 0$:

$$k = \overline{k} e^{2\beta(\overline{Z} - Z)} \text{ and } p = \overline{k}^{-1} e^{\beta(Z + Z_0 - 2\overline{Z})}. \tag{79}$$

This is the case of exponentially graded materials, as given in the literature, for which real fundamental solutions, as expressed in Eqs. (77) and (78) for $h(r)$ and above, for $p(z)$ and $k(z)$, have already been successfully tested. Equations (74) allow more flexibility in the variation pattern of $k(z)$.

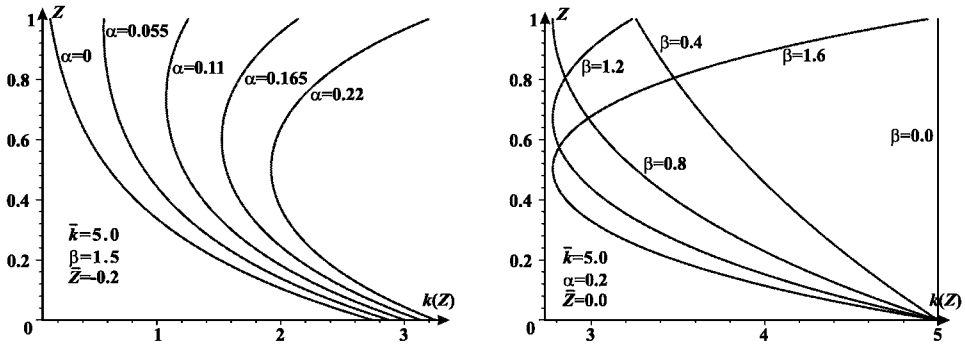


Fig. 2. Illustrative variation patterns of the exponential function $k(z)$, as given in the first of Eqs. (74), for some values of $\alpha$ and $\beta$.

Figure 2 displays some variation patterns of $k(z)$, as given in the first of Eqs. (74), in this first case, for some values of $\alpha$ and $\beta$.

7.2.2. *Second case: solution of the governing equations for* $A = B = 0$

The simpler assumption

$$\begin{aligned} &\frac{p_{,zz}}{p} + \frac{k_{,z}}{k}\frac{p_{,z}}{p} = 0 \\ &\frac{k_{,z}}{k} + 2\frac{p_{,z}}{p} = 0 \end{aligned} \tag{80}$$

has as general solution

$$\begin{aligned} k &= k_0(\alpha Z + 1)^2 \text{ with } k_0 = \overline{k}\left(\alpha \overline{Z} + 1\right)^{-2} \\ p &= p_0(\alpha Z + 1)^{-1} \text{ with } p_0 = k_0^{-1}(\alpha Z_0 + 1)^{-1}, \end{aligned} \tag{81}$$

in terms of material constants $\alpha$ and $\overline{k}$. The constant $\overline{k}$ is expressed in such a way that $k(\overline{z}) = \overline{k}$. As in the first case, $k(z)$ is explicitly expressed as a function of $Z \equiv z + Z_0$, in order to always represent the same material description regardless of local coordinate reference. The parameter $p_0$ is evaluated according to the same type of considerations of the first case. The material property $k(z)$ varies as a second degree polynomial, which approximately represents and is an alternative to the exponential function of the first case. Notice that $\alpha Z + 1 \neq 0$ is a requirement.

The corresponding equations of $h(r)$ in Eqs. (67) and (71) are solved as:

$$h_{,rr} + \frac{2}{r}h_{,r} = 0 \Longrightarrow h = \frac{-1}{4\pi r} \text{ for 3D problems,} \tag{82}$$

$$h_{,rr} + \frac{1}{r}h_{,r} = 0 \Longrightarrow h = \frac{-\ln(r)}{2\pi} \text{ for 2D problems.} \tag{83}$$

The integration constants of the solutions above were evaluated in order to enable the homogeneous solution to be obtained as $\alpha \to 0$, and to correspond to a unitary concentrated source applied at $r = 0$ regardless of the value of $\alpha$.

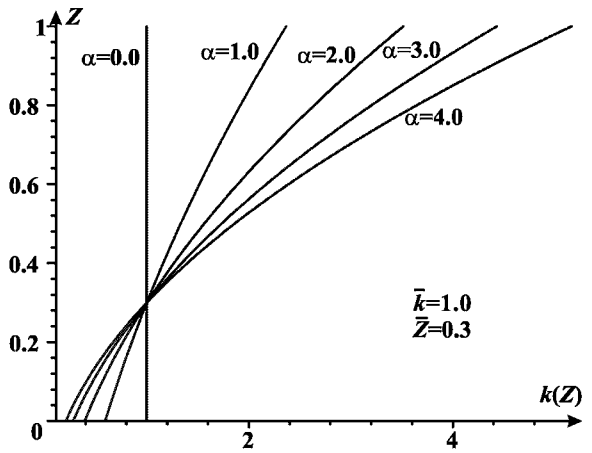


Fig. 3. Illustrative variation patterns of the polynomial function $k(z)$, as given in the first of Eqs. (81), for some values of $\alpha$.

Figure 3 displays some variation patterns of $k(z)$, as given in the first of Eqs. (81), in this second case, for some values of $\alpha$.

7.2.3. *Third case: solution of the governing equations for* $A = \beta^2 > 0, B = 0$

An assumption that is an alternative to the first case is given by a signal change:

$$\begin{aligned} &\frac{p_{,zz}}{p} + \frac{k_{,z}}{k}\frac{p_{,z}}{p} = \beta^2 \\ &\frac{k_{,z}}{k} + 2\frac{p_{,z}}{p} = 0. \end{aligned} \tag{84}$$

The general solution of these equations is

$$\begin{aligned} k &= k_0[\alpha \sin(\beta Z) + \cos(\beta Z)]^2 \text{ with } k_0 = \overline{k}\left[\alpha \sin(\beta \overline{Z}) + \cos(\beta \overline{Z})\right]^{-2} \\ p &= p_0[\alpha \sin(\beta Z) + \cos(\beta Z)]^{-1} \text{ with } p_0 = k_0^{-1}[\alpha \sin(\beta Z_0) + \cos(\beta Z_0)]^{-1}, \end{aligned} \tag{85}$$

in terms of material constants $\alpha$, $\beta$ and $\overline{k}$. Observe that a coordinate translation is also possible in this material model, since constants $\alpha$ and $\beta$ have been adjusted in order to express $k(z)$ as a function of $Z \equiv z + Z_0$. The corresponding equations of $h(r)$ in Eqs. (67) and (71) are:

$$h_{,rr} + \frac{2}{r}h_{,r} + \beta^2 h = 0 \Longrightarrow h = \frac{-\cos(\beta r)}{4\pi r} \text{ for 3D problems,} \tag{86}$$

$$h_{,rr} + \frac{1}{r}h_{,r} + \beta^2 h = 0 \Longrightarrow h = \frac{\mathrm{Y}_0(\beta r)}{4} + \frac{\left[\ln(\frac{\beta}{2}) + \gamma\right]\mathrm{J}_0(\beta r)}{2\pi} \text{ for 2D problems,} \tag{87}$$

where $\mathrm{J}_0$ and $\mathrm{Y}_0$ are Bessel functions of order zero. Similarly to the previous cases, the integration constants of the solutions above have been evaluated in order that the potential field corresponds to a unitary concentrated source applied at $r = 0$.

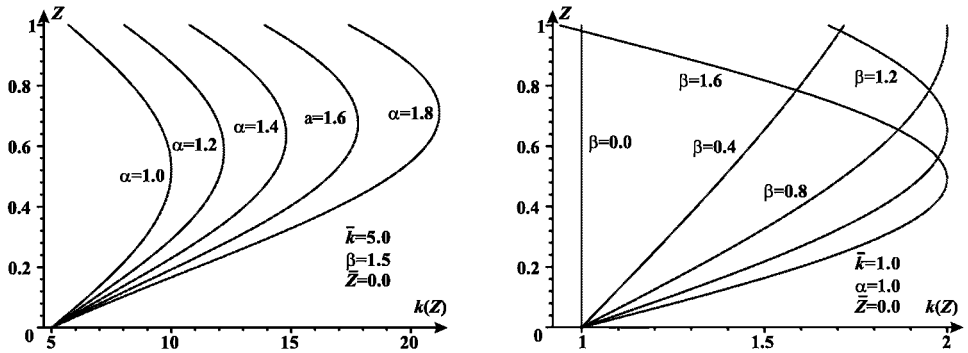


Fig. 4. Illustrative variation patterns of the trigonometric function $k(z)$, as given in the first of Eqs. (85), for some values of $\alpha$ and $\beta$.

Figure 4 displays some variation patterns of $k(z)$, as given in the first of Eqs. (85), in this third case, for some values of $\alpha$ and $\beta$.

7.2.4. *Solution of the governing equations for other cases:* $B \neq 0$

The most general set of assumptions for Eqs. (72),

$$\frac{p_{,zz}}{p} + \frac{k_{,z}}{k}\frac{p_{,z}}{p} = \pm\beta^2$$
$$\left(\frac{k_{,z}}{k} + 2\frac{p_{,z}}{p}\right) z = \lambda \neq 0. \tag{88}$$

admit the solutions listed in Table 1 as cases # 4 - 6. Although real mathematical solutions are found, as summarized in Table 1, they correspond to material variation parameters $k(z)$ that cannot be expressed as a function of $Z \equiv z + Z_0$ and are disregarded as valid FGM fundamental solutions.

### 7.3. *Numerical implementation for 2D potential problems*

For all three cases outlined in the previous Section, a numerical implementation for two-dimensional problems requires the evaluation of the potential $u^*$ in polar coordinates, according to Eq. (70). The flux in the coordinate directions is given as

$$q_r = -k(z)\frac{\partial u^*}{\partial r}, q_\theta = -k(z)\frac{\partial u^*}{\partial \theta} \tag{89}$$

from which it is straightforward to build up the flux normal to the boundary of a numerically discretized material:

$$q = -q_r\frac{\partial r}{\partial \eta} - q_\theta\frac{\partial \theta}{\partial \eta}, \tag{90}$$

for $\eta$ the unitary vector normal to the boundary.

For two-dimensional problems (cases 1 and 3), the expression of $u^*$ involves Bessel functions. An adequate numerical implementation requires expanding $u^*$, $q_r$ and $q_\theta$ in series of the material parameter $\beta$ in order to explicitly consider the logarithm term in the numerical evaluation of the matrices $\mathbf{F}$, $\mathbf{H}$, according to Eq. (23), and $\mathbf{C}^*$, Eq. (47), whenever the integration interval comprises the origin. For the sake of illustration, the expanded expression of $u^*$ reads, in case 1:

$$u^* = p\left[\frac{\beta^2 r^2}{4} + \frac{3\beta^4 r^4}{128} + \frac{11\beta^6 r^6}{13824} - \left(1 + \frac{\beta^2 r^2}{4} + \frac{\beta^4 r^4}{64} + \frac{\beta^6 r^6}{2304}\right)\ln(r) + O(\beta^8)\right]. \tag{91}$$

The terms not affected by $\ln(r)$ are polynomials that multiply the regular function $p$ of Eq. (74), accurately evaluated via a Gauss-Legendre quadrature. Observe that necessarily $k(z) > 0$ in the domain. For the flux $q$ in Eq. (90), there is a $1/r$ singularity, as related to a homogeneous material. Its numerical evaluation has been dealt with sufficiently well in the technical literature.

## 8. Numerical Examples Using Patch Tests

### 8.1. *Irregular-shaped bounded domain with exponentially varying material property*

In the first patch test, a potential source is applied at the indicated point of global coordinates (0.8, 0.2), in the upper left of Fig. 5, thus generating a potential field $u^*$ given by Eq. (70), for a material with $k(z)$ varying exponentially, according to case 1 of Subsection 7.2.1, as summarized in Table 1. The material parameters are $\alpha = 0.215$, $\beta = 1.5$ and $\overline{k} = 5.0$, for the reference coordinate $\overline{Z} = 0.2$, as given by the diagram in the upper left of Fig. 5. Next, one cuts out the contour indicated in the same figure and applies the effects of the potential field along the boundary, considering mesh discretizations with a total of either 15 or 38 almost equally spaced linear elements along the boundary. Since the numerical results with the variational hybrid boundary element method outlined in Section 4 are almost indistinguishable from the results with the simplified version of Section 5, the latter method has been applied in all examples. In the present example, one imposes Dirichlet boundary conditions, with nodal potentials $\mathbf{d}$ given directly from the applied source $u^*$, which enables evaluating the force parameters $\mathbf{p}^*$, according to Eq. (44), and directly expressing results at internal points, according to Eqs. (43) and (3), in absence of body sources.[27,31] In the next three plots of Fig. 5, potential and fluxes in the directions $x$ and $z$,

$$q_x = \frac{x}{r}q_r - \frac{z}{r^2}q_\theta, q_z = \frac{z}{r}q_r - \frac{x}{r^2}q_\theta, \tag{92}$$

as evaluated along the interior dash line segment indicated in the figure for each one of the discretizations implemented, are displayed for comparison with the analytical values.

Table 1. Summary of all 2D and 3D existing solutions of a problem of potential for an FGM in terms of assumed constants $A$ and $B$ in Eq. (72). Bessel functions of first and second kind and generic order are used in some cases. Solutions for cases # 4-6, although mathematically possible, refer to unfeasible material properties $k(z)$, as coordinate translation, for considering different local systems in Fig. 1, is not supported by the integration constants.

| Case # | Assumed constants | Solutions of functions $p$ and $k$ in Eq. (72) | | Solutions of function $h$ in Eqs. (67) and (71) |
|---|---|---|---|---|
| 1 | $A=-\beta^2$<br>$B=0$ | $k=k_0e^{-2\beta Z}\left(\alpha e^{2\beta Z}+1\right)^2, k_0=\overline{k}e^{2\beta\overline{Z}}\left(\alpha e^{2\beta\overline{Z}}+1\right)^{-2}$<br>$p=p_0e^{\beta Z}\left(\alpha e^{2\beta Z}+1\right)^{-1}, p_0=k_0^{-1}e^{\beta Z_0}\left(\alpha e^{2\beta Z_0}+1\right)^{-1}$ | 2D<br>3D | $h=\{\mathrm{K}_0(\beta r)+[\ln(\beta/2)+\gamma]\,\mathrm{I}_0(\beta r)\}/2\pi$<br>$h=-\cosh(\beta r)/4\pi r$ |
| 2 | $A=0$<br>$B=0$ | $k=k_0(\alpha Z+1)^2, k_0=\overline{k}\left(\alpha\overline{Z}+1\right)^{-2}$<br>$p=p_0(\alpha Z+1)^{-1}, p_0=k_0^{-1}(\alpha Z_0+1)^{-1}$ | 2D<br>3D | $h=-\ln(r)/2\pi$<br>$h=-1/4\pi r$ |
| 3 | $A=\beta^2$<br>$B=0$ | $k=k_0[\alpha\sin(\beta Z)+\cos(\beta Z)]^2$<br>$k_0=\overline{k}\left[\alpha\sin(\beta\overline{Z})+\cos(\beta\overline{Z})\right]^{-2}$<br>$p=p_0[\alpha\sin(\beta Z)+\cos(\beta Z)]^{-1}$<br>$p_0=k_0^{-1}[\alpha\sin(\beta Z_0)+\cos(\beta Z_0)]^{-1}$ | 2D<br>3D | $h=\mathrm{Y}_0(\beta r)/4+[\ln(\beta/2)+\gamma]\,\mathrm{J}_0(\beta r)/2\pi$<br>$h=-\cos(\beta r)/4\pi r$ |
| 4 | $A=0$<br>$B=\lambda$ | $k=k_0z^\lambda\left(\alpha z^{1-\lambda}+1\right)^2$ †<br>$p=p_0\left(\alpha z^{1-\lambda}+1\right)^{-1}$ | 2D<br>3D | $h=C_1+C_2r^{-\lambda}$<br>$h=C_1+C_2r^{-1-\lambda}$ |
| 5 | $A=\beta^2$<br>$B=\lambda$ | $k=k_0z\left[\alpha\mathrm{J}_{(\lambda-1)/2}(\beta z)+\mathrm{Y}_{(\lambda-1)/2}(\beta z)\right]^2$ †<br>$p=p_0z^{(\lambda-1)/2}\left[\alpha\mathrm{J}_{(\lambda-1)/2}(\beta z)+\mathrm{Y}_{(\lambda-1)/2}(\beta z)\right]^{-1}$ | 2D<br>3D | $h=r^{-\lambda/2}\left[C_1\mathrm{Y}_{\lambda/2}(\beta r)+C_2\mathrm{J}_{\lambda/2}(\beta r)\right]$<br>$h=r^{-(\lambda+1)/2}\left[C_1\mathrm{Y}_{(\lambda+1)/2}(\beta r)+C_2\mathrm{J}_{(\lambda+1)/2}(\beta r)\right]$ |
| 6 | $A=-\beta^2$<br>$B=\lambda$ | $k=k_0z\left[\alpha\mathrm{I}_{(\lambda-1)/2}(\beta z)+\mathrm{K}_{(\lambda-1)/2}(\beta z)\right]^2$ †<br>$p=p_0z^{(\lambda-1)/2}\left[\alpha\mathrm{I}_{(\lambda-1)/2}(\beta z)+\mathrm{K}_{(\lambda-1)/2}(\beta z)\right]^{-1}$ | 2D<br>3D | $h=r^{-\lambda/2}\left[C_1\mathrm{K}_{\lambda/2}(\beta r)+C_2\mathrm{I}_{\lambda/2}(\beta r)\right]$<br>$h=r^{-(\lambda+1)/2}\left[C_1\mathrm{K}_{(\lambda+1)/2}(\beta r)+C_2\mathrm{I}_{(\lambda+1)/2}(\beta r)\right]$ |

†Physically meaningless

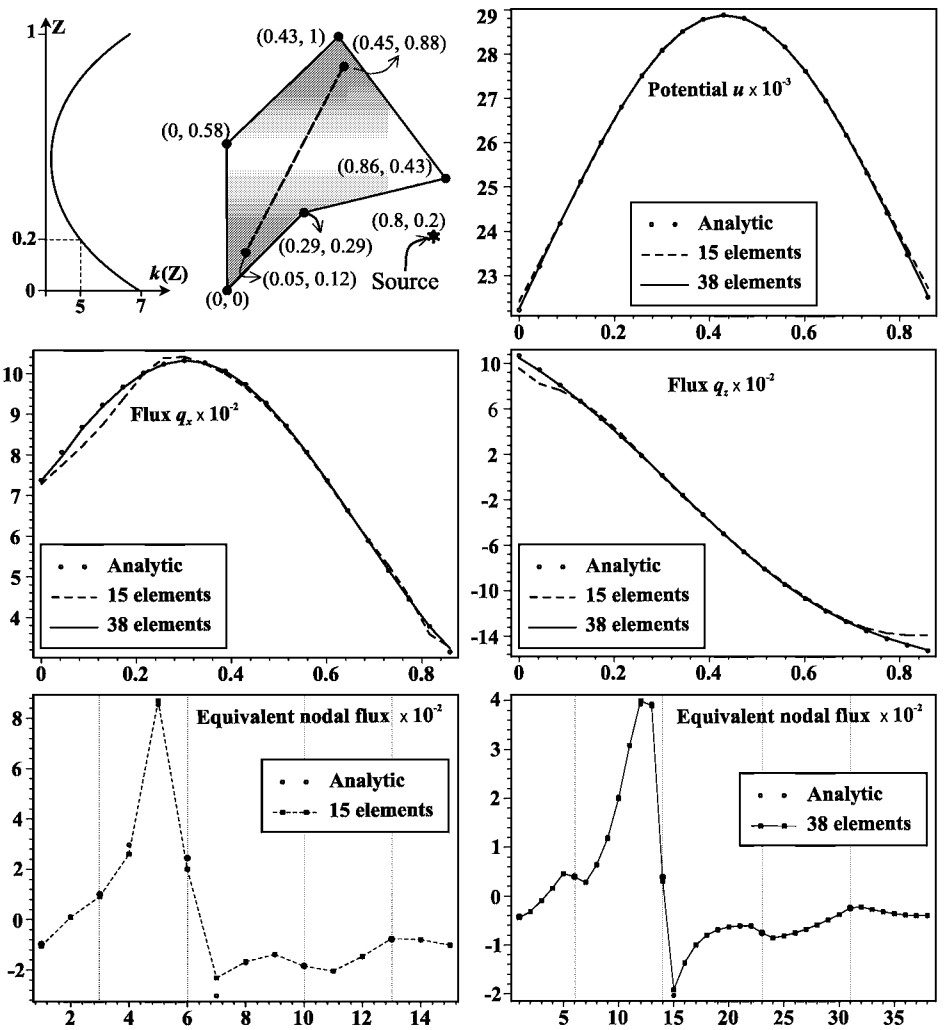


Fig. 5. Upper left: scheme of function $k(z)$ varying exponentially for $\alpha = 0.215$, $\beta = 1.5$, $\overline{k} = 5.0$, $\overline{Z} = 0.2$ and irregular contour with indicated singular source; remaining graphics: values of potential and fluxes along a line segment and equivalent nodal fluxes for two meshes, as compared with the analytical results.

The remaining two plots at the bottom of Fig. 5 display, for each discretized mesh, equivalent nodal fluxes evaluated along the boundary nodes as the vector $\mathbf{p}$ in Eq. (39). The analytical values are obtained as the vector $\mathbf{p}$ in Eq. (18), for $\overline{q}$ the normal flux corresponding to the applied source $u^*$. In the plots, vertical lines separate each one of the five straight boundary segments of the cut-out, displayed counterclockwise starting from the origin.

This kind of patch test is very useful because an irregularly-shaped model is submitted to high gradients and nonetheless an analytical solution is available

to compare with. Although in this and in the following examples only Dirichlet boundary conditions have been considered, Neumann boundary conditions, as well as general mixed boundary conditions can be easily simulated in the patch tests and lead to similar convergence patterns.[27] It is worth noticing that, although for Dirichlet boundary conditions the second of Eqs. (49) is not required, as long as one is only interested in results at internal points, the evaluation of matrix $\mathbf{H}$ is implicit in the first of Eqs. (49), since the matrix $\mathbf{V}$ has to be obtained according to Eq. (29) in order to enable determining the main-diagonal elements of $\mathbf{U}^*$ in Eq. (48). Moreover, the displayed numerical comparison of equivalent nodal fluxes explicitly makes use of all equations involved in the problem, thus almost exhausting the possibilities of testing the formulation, in this example.

#### 8.1.1. *Example with mixed boundary conditions*

Owing to its variational basis, the hybrid boundary element method considers Neumann-type boundary conditions in terms of equivalent nodal fluxes obtained by virtual work. As a consequence, discrepancies in terms of numerical and analytical nodal fluxes about corner nodes may be observed. The same kind of problem occurs in the (displacement) finite element method, although it may be avoided, or at least alleviated, in the conventional boundary element method. Then, it is expected that imposition of Neumann-type boundary conditions leads to less accurate results in a numerical simulation, as compared with imposition of Dirichlet boundary conditions. For the sake of illustration, Fig. 6 presents the same example of Fig. 5, except that, given the applied source, potential values are prescribed only along the two first straight boundary segments (starting counterclockwise from the origin), whereas fluxes are applied along the remaining three segments (dotted border). To compare the accuracy of the results, the plots of Fig. 6 display the same kind of results of the corresponding ones of Fig. 5. Although visually almost imperceptible, the results of Fig. 6 are less accurate.

### 8.2. *Irregularly shaped cavity in an infinite domain – Exponentially graded medium*

In the second example, the same irregular contour (cf previous Section) is considered as a cavity in an unbounded domain. A potential source is placed at the indicated point of global coordinates (0.5, 0.7), in the upper left corner of Fig. 7, generating a potential field $u^*$ given by Eq. (70), for a material with $k(z)$ varying exponentially, according to case 1 of Subsection 7.2.1, as summarized in Table 1. Material properties are $\alpha = 0$, $\beta = 1.8$ and $\overline{k} = 5$, for the reference coordinate $\overline{Z} = -0.05$. Mesh discretizations are the same of the first example.[27,31] This time, potential as well as $x$ and $z$ gradients are evaluated along the external dash line segment of the figure and displayed in the remaining three plots and compared with the analytical values. Equations (60), (54) and (3) are used in the numerical evaluations, in the absence of body sources.

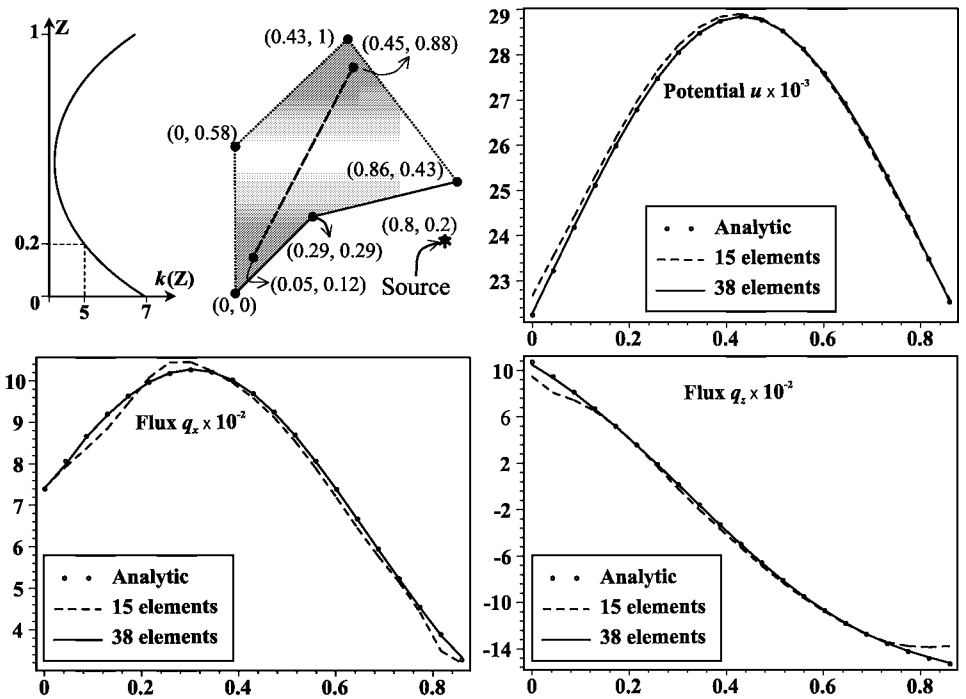


Fig. 6. Same example of Fig. 5, as described in Subsection 8.1, but considering prescribed fluxes along the boundary segments marked by dotted lines; remaining graphics: values of potential and fluxes along a line segment, as compared with the analytical results.

The remaining two plots at the bottom of Fig. 7 display, for each discretized mesh, equivalent nodal fluxes evaluated along the boundary nodes as the vector $\overline{\mathbf{p}}$ of Eq. (60) (clockwise) integrated as $\mathbf{p}$ in Eq. (39). The analytical values are obtained as the vector $\mathbf{p}$ in Eq. (18), for $\overline{q}$ the normal flux corresponding to the applied source $u^*$, exactly as in the previous example, but using clockwise integration. In the plots, vertical lines separate each one of the five straight boundary segments of the cut-out, displayed counterclockwise starting from the origin. Once again, convergence of results and good accuracy is achieved.

### 8.3. *Multiply connected, irregularly shaped domain – Polynomially graded medium*

A multiply connected, irregularly shaped domain is considered, as illustrated in the upper left of Fig. 8. A potential source is placed at global coordinates (0.48, 0.34), thus internal to the cut-out, generating a potential field $u^*$ given by Eq. (70), for a material with $k(z)$ varying according to the polynomial pattern of case 2 of Subsection 7.2.2, as summarized in Table 1. Material properties are $\alpha = 4.5$ and $\overline{k} = 50$, for the reference coordinate $\overline{Z} = 1.85$. Mesh discretizations use 47 and 78 linear elements, of which 10 and 20 elements, respectively, approximate the internal

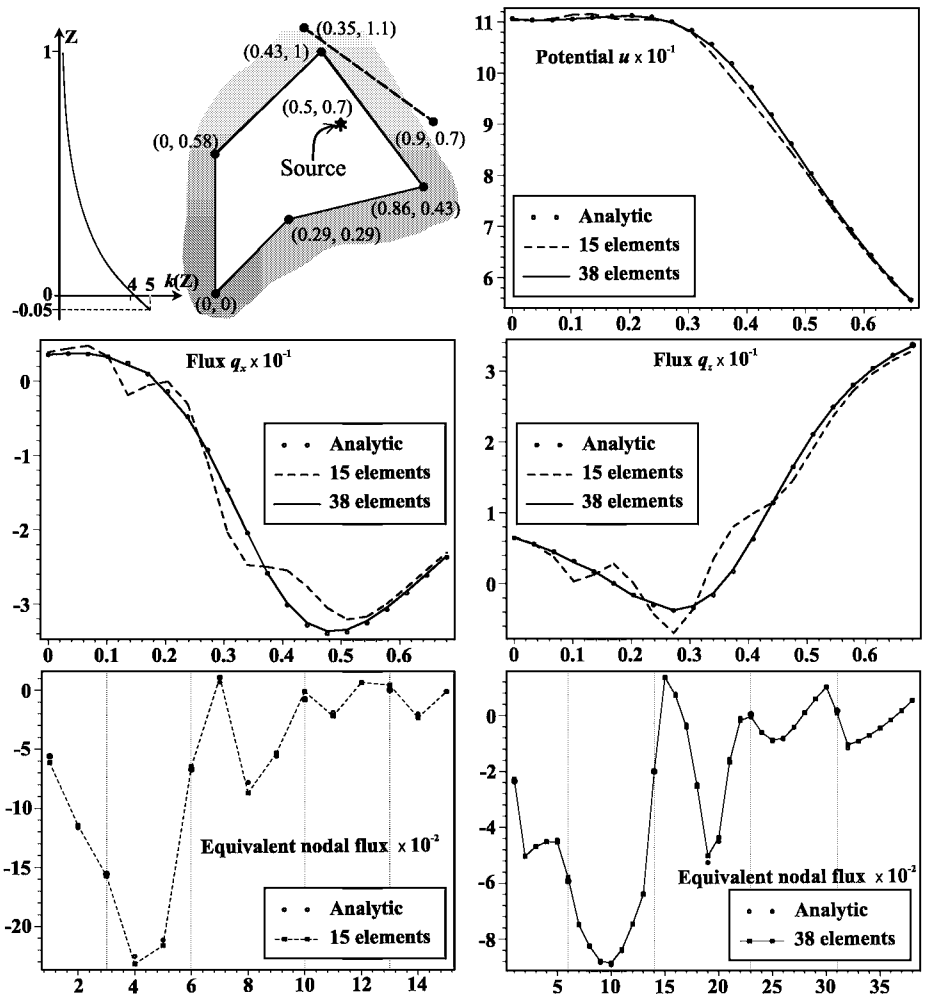


Fig. 7. Upper left: scheme of function $k(z)$ varying exponentially for $\alpha = 0$, $\beta = 1.8$, $\overline{k} = 5$, $\overline{Z} = -0.05$ and irregular contour for a cavity, with indicated singular source; remaining graphics: values of potential and fluxes along a line segment and equivalent nodal fluxes for two meshes, as compared with the analytical results.

circle.[27] Superposition of effects for bounded and unbounded domains is used in the numerical evaluations, combining the equations of Sections 5 and 6.

Following the previous schemes, potential as well as $x$ and $z$ gradients are evaluated along the dashed line segment of the figure and displayed in the remaining three plots, for comparison with the analytical values. Moreover, the remaining two plots at the bottom of Fig. 8 compare numerical and analytical values of equivalent nodal fluxes, as done for previous examples. The results for the internal circle are given as disconnected sets on the right-hand-side of the plots. Once again, convergence of results and good accuracy is achieved, particularly considering the high

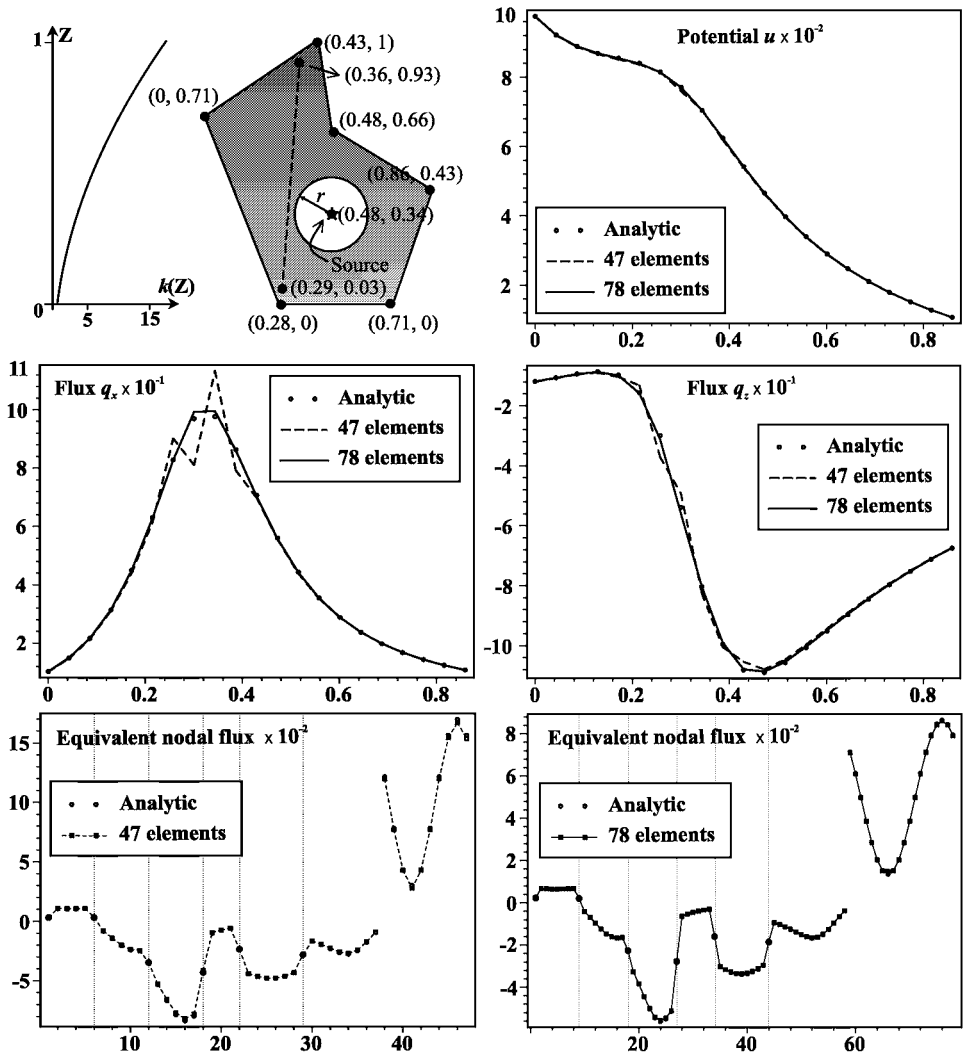


Fig. 8. Upper left: scheme of function k(z) varying polynomially for $\alpha = 4.5$, $\overline{k} = 50$, $\overline{Z} = 1.85$ and irregular contour for a multiply connected domain (radius of circular hole is $r = .14$), with indicated singular source; remaining graphics: values of potential and fluxes along a line segment and equivalent nodal fluxes for two meshes, as compared with the analytical results.

gradients introduced and that some results have been evaluated in the vicinity of the internal boundary.

### 8.4. *Multiply connected, irregularly shaped domain – Trigonometrically graded medium*

A multiply connected, irregularly shaped domain is considered, as illustrated in the upper left corner of Fig. 9. A potential source is placed external to the cut-out, at the

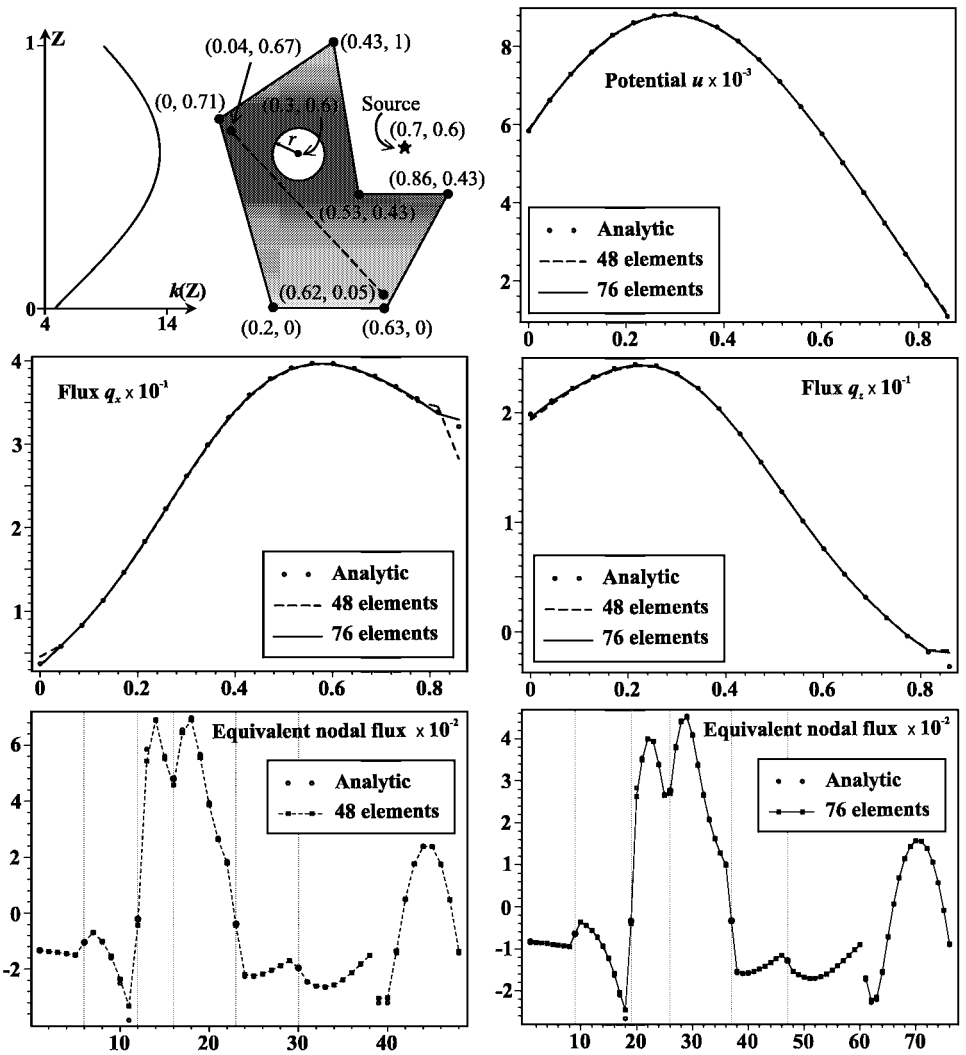


Fig. 9. Upper left: scheme of function $k(z)$ varying trigonometrically with $\alpha = 1.25$, $\beta = 1.5$, $\overline{k} = 5$, $\overline{Z} = 1.2$ and irregular contour for a multiply connected domain (radius of circular hole is $r = .1$), with indicated singular source; remaining graphics: values of potential and fluxes along a line segment and equivalent nodal fluxes for two meshes, as compared with the analytical results.

indicated point of global coordinates (0.7, 0.6), generating a potential field $u^*$ given by Eq. (70), for a material with $k(z)$ varying trigonometrically, according to case 3 of Subsection 7.2.3, as summarized in Table 1. Material properties are $\alpha = 1.25$, $\beta = 1.5$ and $\overline{k} = 5$ for the reference coordinate $\overline{Z} = 1.2$. Mesh discretizations use 48 and 76 linear elements, of which 10 and 16 elements, respectively, approximate the internal circle.[27] Superposition of effects for bounded and unbounded domains is used in the numerical evaluation, combining the equations of Sections 5 and 6.

Potential, as well as $x$ and $z$ gradients, are evaluated along the dash line segment of the figure and displayed in the remaining three plots of Fig. 9 for comparison with the analytical values. The remaining two plots at the bottom of Fig. 9 compare numerical and analytical values of equivalent nodal fluxes, as done for the previous examples. The results for the internal circle are given as a disconnected set on the right-hand-side of the plots. Once again, convergence of results and good accuracy is achieved.

## 9. Concluding Remarks

The hybrid boundary element method, both in its variational and its simplified versions, is extended to potential problems involving nonhomogeneous materials. As schematically displayed as cases # 1-3 in Table 1 and illustrated in Figs. 3-5, the present formulation considers a wide range of material properties $k(z)$, which may vary either exponentially, polynomially or trigonometrically. Several generalized patch tests validate the theoretical formulations for bounded, unbounded and multiply connected domains, including mixed boundary conditions. Future work includes extension of the hybrid boundary element method to elasticity problems in FGMs.

## Acknowledgements

This collaborative project was supported by the Brazilian agencies FAPERJ and CNPq, and the American agency NSF through grant CMS-0115954. Any opinions, findings, conclusions or recommendations expressed in this publication are those of the authors and do not necessarily reflect the views of the sponsors.

## References

1. T. H. H. Pian, in *Proc. Conf. on Matrix Meths. in Struct. Mech.*, AFFDL-TR-66-80, Wright Patterson Air Force Base, Ohio, p. 457 (1966).
2. N. A. Dumont, in *Boundary Element Techniques: Applications in Fluid Flow and Computational Aspects*, ed. C. A. Brebbia and W. Venturini, Computational Mechanics Publications, Adlard and Son Ltd., Southampton, p. 225 (1987).
3. N. A. Dumont, *Applied Mechanics Reviews*, **42**, Nr. 11, Part 2, p. S54 (1989).
4. N. A. Dumont, and R. Oliveira, *Int. J. of Sol. Struct.*, **38**, Issue 10-13, p. 1813 (2001).
5. N. A. Dumont, and A. A. O. Lopes, *Fatigue & Fracture of Engineering Materials & Structures*, Vol. 26, p. 151 (2003).
6. N. A. Dumont, M. U. Quintana Cossio, *Building Research Journal*, **49**, Nr. 1, p. 35 (2001).
7. L. Gaul, M. Wagner, W. Wenzel, and N. A. Dumont, *Int. J. of Sol. Struct.*, **38**, Issue 10-13, p. 1871 (2001).
8. R. A. P. Chaves, *Study of the Hybrid Boundary Element Method and Proposition of a Simplified Formulation*, M.Sc. Dissertation (in Portuguese), PUC-Rio, Brazil (1999).
9. N. A. Dumont, and R. A. P. Chaves, in *Book of Abstracts 5th U.S. National Congress on Computational Mechanics (Minisymposium Advances in Boundary Element Methods)*, p. 68, University of Colorado, Boulder, USA, (1999).

10. N. A. Dumont, and R. A. P. Chaves, in *XX CILAMCE - 20th Iberian Latin American Congress on Computational Methods in Engineering*, in CD-ROM, So Paulo, Brazil (1999).
11. N. A. Dumont, and R. A. P. Chaves, in *XXI CILAMCE - 21st Iberian Latin American Congress on Computational Methods in Engineering*, in CD-ROM, Rio de Janeiro, Brazil (2000).
12. E. M. Carrillo-Heian, R. D. Carpenter, G. H. Paulino, J. C. Gibeling, and Z. A. Munir, *Journal of the American Ceramic Society* **84**, Nr. 5, p. 962 (2001).
13. M. Tokita, *Materials Science Forum*, 308-311, p. 83 (1999).
14. S. Suresh, and A. Mortensen, *Fundamentals of Functionally Graded Materials*, Institute of Materials, IOM Communications Ltd., London (1998).
15. Y. Miyamoto, W. A. Kaysser, B. H. Rabin, A. Kawasaki, and R. G. Ford, *Functionally Graded Materials: Design, Processing and Applications*, Kluwer Academic Publishers, Dordrecht, The Netherlands (1999).
16. G. H. Paulino Z.-H. Jin, and R. H. Dodds Jr., in Comprehensive Structural Integrity, Vol.2, edited by B. Karihaloo and W. G. Knauss (Elsevier, 2003) p. 607.
17. Y.-S. Chan, G. H. Paulino, and A. C. Fannjiang, *Int. J. of Sol. Struct.*, **38**, Nr. 17, p. 2989 (2001).
18. P. A. Martin, J. D. Richardson, L. J. Gray, and J. Berger, *Proceedings of the Royal Society of London Series A: Mathematical, Physical and Engineering Sciences*, **458**, Nr.2024, p.1931 (2002).
19. Y.-S. Chan, L.J. Gray, T. Kaplan, and G. H. Paulino, *Proceedings of the Royal Society of London Series A: Mathematical, Physical and Engineering Sciences*, **460**, Nr.2046, p.1689 (2004).
20. L. J. Gray, T. Kaplan, J. D. Richardson, and G. H. Paulino, *ASME Journal of Applied Mechanics*, Vol. 70, Nr. 4, p. 543 (2003).
21. S. I. Georghitza, In *First Symposium on the Fundamentals of Transport Phenomena in Porous Media*, Int. Assoc. Hydraul. Res., Haifa, Israel (1969).
22. J. Bear, *Dynamics of Fluids in Porous Media*, Elsevier, New York (1972).
23. A. H.-D. Cheng, *Water Resources Research*, **20**, Nr. 7, p. 980 (1984).
24. A. H.-D. Cheng, in *Topics in Boundary Element Research, Volume 4 Applications in Geomechanics, Chapter 6*, ed. C. A. Brebbia, p. 129, Springer-Verlag, Berlin (1987).
25. A. Sutradhar and G. H. Paulino *International Journal for Numerical Methods in Engineering*, **60**, Nr.13, p.2203 (2004).
26. A. Sutradhar and G. H. Paulino *Computer Methods in Applied Mechanics and Engineering*, **193**, Nrs.42-44, p.4511 (2004).
27. R. A. P. Chaves, *The Simplified hybrid boundary element method applied to time-dependent problems*, Ph.D. Thesis (in Portuguese), PUC-Rio, Brazil (2003).
28. A. Ben-Israel, and T. N. E. Greville, *Generalized Inverses: Theory and Applications*, Krieger, New York (1980).
29. N. A. Dumont, in *Computer Assisted Mechanics and Engineering Sciences*, Vol. 10, p. 407 (2003).
30. N. A. Dumont, R. A. P. Chaves, and G. H. Paulino, in *Computational Mechanics - New Frontiers for the New Millenium*, eds. S. Valliappan, and N. Khalili, Elsevier Science Ltd, p. 1019 (2001).
31. N. A. Dumont, R. A. P. Chaves, and G. H. Paulino, in *Boundary Elements XXIV - Incorporating Meshless Solutions*, eds. C. A. Brebbia, A. Tadeu, and V. Popov, WIT Press, Southampton, p. 267 (2002).